

A symmetry-orientated divide-and-conquer method for crystal structure prediction

Cite as: J. Chem. Phys. 156, 014105 (2022); doi: 10.1063/5.0074677

Submitted: 10 October 2021 • Accepted: 5 December 2021 •

Published Online: 3 January 2022



View Online



Export Citation



CrossMark

Xuecheng Shao,¹ Jian Lv,¹ Peng Liu,¹ Sen Shao,¹ Pengyue Gao,¹ Hanyu Liu,¹ Yanchao Wang,^{1,2,a)} , and Yanming Ma^{1,2,3,b)}

AFFILIATIONS

¹ International Center of Computational Method and Software, College of Physics, Jilin University, Changchun 130012, China

² State Key Laboratory of Superhard Materials, College of Physics, Jilin University, Changchun 130012, China

³ International Center of Future Science, Jilin University, Changchun 130012, China

^{a)}Author to whom correspondence should be addressed: wyc@calypso.cn

^{b)}Electronic mail: mym@jlu.edu.cn

ABSTRACT

Crystal structure prediction has been a subject of topical interest but remains a substantial challenge especially for complex structures as it deals with the global minimization of the extremely rugged high-dimensional potential energy surface. In this paper, a symmetry-orientated divide-and-conquer scheme was proposed to construct a symmetry tree graph, where the entire search space is decomposed into a finite number of symmetry dependent subspaces. An artificial intelligence-based symmetry selection strategy was subsequently devised to select the low-lying subspaces with high symmetries for global exploration and in-depth exploitation. Our approach can significantly simplify the problem of crystal structure prediction by avoiding exploration of the most complex P_1 subspace on the entire search space and has the advantage of preserving the crystal symmetry during structure evolution, making it well suitable for predicting the complex crystal structures. The effectiveness of the method has been validated by successful prediction of the candidate structures of binary Lennard-Jones mixtures and the high-pressure phase of ice, containing more than 100 atoms in the simulation cell. The work therefore opens up an opportunity toward achieving the long-sought goal of crystal structure prediction of complex systems.

Published under an exclusive license by AIP Publishing. <https://doi.org/10.1063/5.0074677>

I. INTRODUCTION

Knowledge of crystal structures is essential if the properties of materials are to be understood and exploited, particularly when establishing a correspondence between material performance and their chemical compositions. There is a high interest in crystal structure prediction (CSP), where crystal structures are precisely predicted from theory without acquiring any prior known structure knowledge in case the only given information is the chemical compositions of materials. Thermodynamics plays a critical role in determining the structures and the likelihood of the structures formed in nature associated with their energies. CSP is targeted to identify the energetically most favorable structure that is synthesizable in experiments and whose energy is a global minimum on the potential energy surface (PES), a vast “landscape” in a high-dimensional space that possesses high energy barriers separating energy minima.

Unfortunately, since the analytic form of the PES is unknown, a numerical solution for finding the global minimum is essential. Application of the variable-cell geometry optimization,¹ which is commonly used in modern CSP methods,^{2–6} simplifies the targeted PES from a continuous landscape into discrete energy minima. However, the number of energy minima is still an astronomical figure (e.g., it is roughly estimated to be 10^{42} for a system of 100-atom Lenard-Jones cluster⁷) and scales exponentially with the number of atoms in a structure. Mathematically, global minimization among these energy minima is a nondeterministic polynomial-time hard problem, posing a grand challenge for CSP.⁸

A variety of popular CSP methods (see, e.g., Ref. 9 for details on the different methods) were recently developed and successfully applied to solve structure-related problems, leading to a number of major discoveries (e.g., the finding of pressure stabilized high-temperature superconductor LaH_{10} that holds the record high T_c at 260 K known thus far^{10,11}). These methods were proposed based

on various sampling schemes on PES, including the simulated annealing,¹² basin-hopping,¹³ minima hopping,¹⁴ metadynamics,¹⁵ random sampling,³ genetic algorithm,^{16–20} and swarm-intelligence algorithm.^{24,5} These methods use different structure searching schemes but share a common strategy: direct sampling over the entire PES.²¹ Since the search space is vast as aforementioned and the typical first-principles structure searching simulations can only explore several ten thousand structures or much less, a direct sampling faces inevitably a problem of insufficient sampling, especially for a large system (e.g., structures having >50 atoms in the unit cell).

Crystal structures sitting at PES constitute a vast structure (or configuration) space. A sampling on structure space is mathematically equivalent to sampling on PES. In an effort to avoid the above-mentioned insufficient problem for a direct sampling on PES associating with the spatial arrangements of atoms, we develop a symmetry-orientated divide-and-conquer scheme via the construction of a symmetry tree graph (STG) that allows for a rigorous decomposition of a vast structure space into a number of symmetry dependent structure subspaces and elimination of the most complex P_1 subspace to significantly reduce the complexity of the structure space.²² A symmetry-preserved artificial intelligent

algorithm (SPAI) was subsequently devised to locate the suitable subspaces and further performs in-depth exploitation in the selected promising subspaces. As we will illustrate in more detail in the following, if the stable crystal structure has a high symmetry, high searching efficiency and success rate can be achieved for the current method.

II. METHODS

Description of a crystal structure containing N atoms needs a maximal number of $3N + 3$ degrees of freedom for structural parameters including six for the crystallographic unit cell and $3N - 3$ for atomic positions. The actual number of degrees of freedom depends on the symmetry of a structure. As depicted in Fig. 1(a), for a 100-atom structure, 303 degrees of freedom are required to model a triclinic system, while it is substantially reduced to 23 for a high symmetric cubic system. It is empirically suggested that the search space with a high degree of freedom usually has a large hypervolume²³ on PES, as further supported by the mathematical fact that there is an exponential increase in the number of energy minima $n(d)$ with the number of degrees of freedom (d): $n(d) = e^{\alpha d}$, where

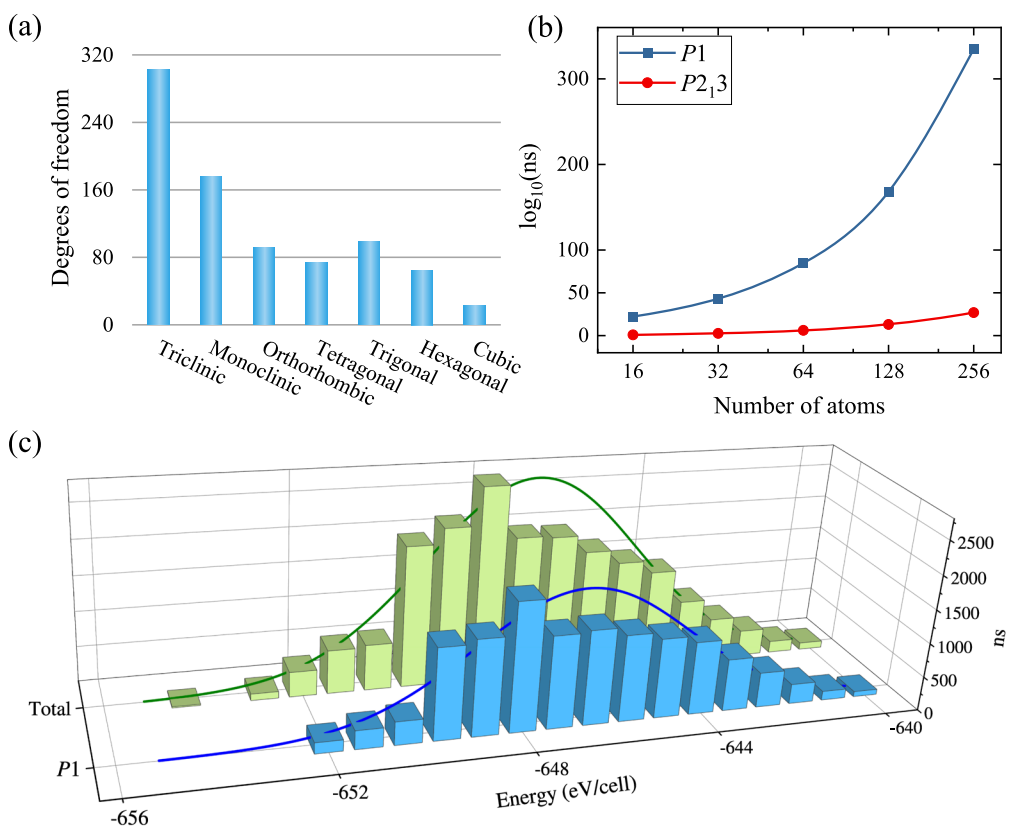


FIG. 1. (a) The maximal number of degrees of freedom to model a crystal structure containing 100 atoms for the choices of different symmetries. (b) The estimated number of structures (ns) in a \log_{10} scale sitting at energy minima vs the various system sizes for P_1 and $P_{2,3}$ symmetries. Note that the system-specific constant of α is set to be 1.0 for both systems. (c) The distribution of 20 000 random structures of MgAl_2O_4 over the energy for all symmetries and P_1 .

α is a system-specific constant.⁸ The dramatic reduction of d for a high symmetric structure results in a substantially reduced $n(d)$ as illustrated in Fig. 1(b), where $n(d)$ for a low symmetric $P1$ structure is compared with that for a high symmetric $P2_{13}$. It is seen that the number of energy minima for a 64-atom system reaches up to $\sim 10^{85}$ for $P1$, whereas it is amazingly reduced to 10^6 for $P2_{13}$.

As described above, the complexity of the structure space originated from the complexity of low symmetric structures. As a result, a direct sampling over the structure space inevitably enhances the visibility of low symmetric structures, whereas high symmetric structures are underrepresented as illustrated by a numerical experiment for 20 000 random structures of MgAl_2O_4 showing 85.85% and 14.15% occupancies for $P1$ and other symmetric structures in Fig. 1(c), respectively. In case that the true structure is having a high symmetry, the problem we face for CSP would be much simplified as we can mainly focus on high symmetric structures. Our wish is not in contradiction with the previous statistical analysis on that the crystal structure is likely with high symmetry.²⁴

Earlier methods^{4,25} that use symmetry for the generation of structures cannot be used for such a purpose since the symmetry is not preserved during structure evolution, leading to enhancement of the visibility of $P1$ structures. While the predefined cell parameters are usually required to preserve symmetry for several genetic algorithms using symmetry-adapted-crossover operations. Thus, these methods can only apply to specific systems (e.g., substitutionally disordered materials).²⁶ We here construct a three-level STG in Fig. 2 to represent the structure space in which crystal structures are grouped into a set of crystal symmetry dependent subspaces (level 1) and site-symmetry related groups (level 2) following the rules of crystallographic symmetry. In level 1, for a three-dimensional crystal, using 230 space groups as subspaces can give a rigorous description of an entire structure space (S) as described by $S = \bigcup_{i=1}^{230} S_i$, where S_i denotes the i th subspace with the i th space group. Each subspace S_i can be further subdivided into a

set of site-symmetry related groups (S_{ij}) in level 2 as described by $S_i = \bigcup_{j=1}^n S_{ij}$. Within each S_{ij} , the structures share the same combination of the Wyckoff positions. The complete list of all possible combinations (n) is mathematically enumerated, and atomic positions in structures can be obtained by coordinate descriptions of the Wyckoff positions, i.e., crystallographic orbits. In level 3, once the crystallographic orbits are determined, the structure space is eventually decomposed into symmetry-cataloged subspaces within which the structures could reduce to a same local minimum structure after the geometry optimizations. One example of STG of MgAl_2O_4 , which has 28 atoms in the cell, was presented in Fig. S1.

With the STG at hand, it is now possible to develop the divide-and-conquer scheme for crystal structure prediction. There is a need of three different agents that allow for proper samplings on the corresponding three different levels in the STG. We name them as scout, onlooker, and employee agents, which are borrowed from the artificial bee colony algorithm.^{27–29} Our method is a population-based evolutionary scheme in which the initial structures in the first population are generated randomly with the symmetry constraints. Note that the candidate structures with $P1$ space group are excluded to reduce the complexity of the structure space. All structures are optimized and ranked in order of their energies as high, middle, and low energy structures that are then assigned as scouts, onlookers, and employees, respectively. Structures in the next population are generated with the aid of all three agents of scout, onlooker, and employee.

The agent scout is responsible for the exploration of 229 subspaces not including $P1$ in level 1 of STG. Scouts are first discarded and then re-generated by randomly choosing space groups to avoid any personal bias on the generation of structure. At the same time, a strict control to avoid the repetition of the same space group has been imposed until all 229 space groups have been examined. These constraints ensure the samplers walk over less-explored space groups for better coverage of the entire structure space. The agent

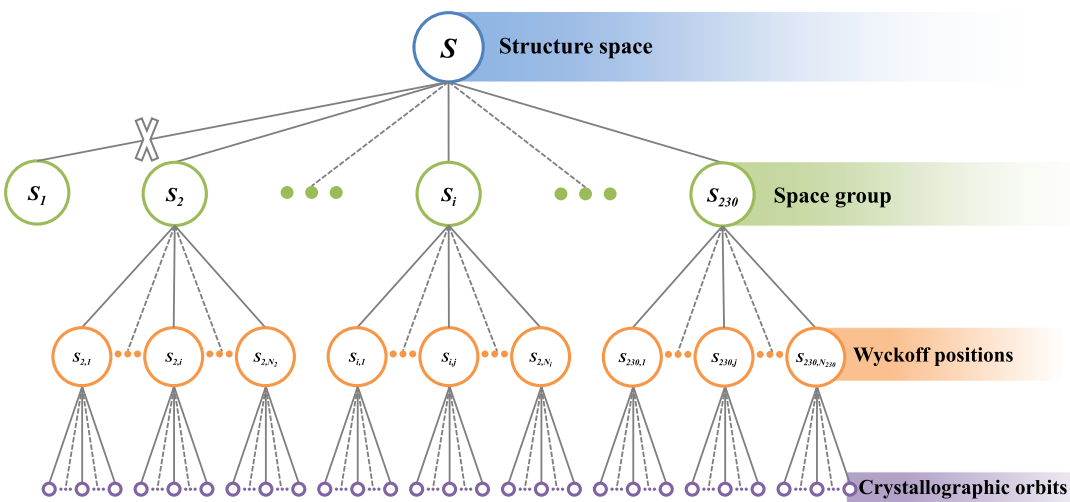


FIG. 2. A schematic representation of STG and SPAI for the exploration of STG. Note that each node in STG is located along a one-dimensional unphysical coordinate simply for visual clarity.

onlooker is responsible for the exploration of site-symmetry related groups in level 2 of STG. With the information of space group unaltered, onlookers randomly choose a different combination of the Wyckoff positions allowed following the probability p_i ,

$$p_i = \frac{fit_i}{\sum_{i=1}^{SN} fit_i}, \quad (1)$$

where SN denotes the number of onlookers and fit_i is evaluated by its energy (E_i),

$$fit_i = \begin{cases} \frac{1}{1 + E_i}, & \text{if } E_i \geq 0, \\ 1 + |E_i|, & \text{if } E_i < 0. \end{cases} \quad (2)$$

The use of probability control ensures that onlookers with lower energies have a higher probability to be selected for the generation of structures in the next population. The agent employee is responsible for the exploration of crystallographic orbits in level 3 of STG. With the information of the space group and site-symmetry group unaltered, employees randomly choose different atomic coordinates of the Wyckoff positions to generate structures in the next population. Our structure searching scheme is controlled in a self-organized manner, and the roles of three agents can dynamically change depending on the order of their energies. When an employee cannot be further improved within certain predetermined cycles, it automatically becomes a scout, whereas a scout with lower energy can change its role as an employee or onlooker. The structural variations of the onlooker and employee act, from the point of view of the entire population, as feedback, amplify the promising structure space by sharing their crystallographic information, and ensure the structures in the population evolve positively by performing more attempts nearby the low-lying structure space.

Besides the general structure prediction packages, there are also some very powerful open-source programs (e.g., RandSpg³⁰ and

PyXtal³¹) that can create random symmetric crystals. Our method can be easily implemented in these programs. Here, we implemented our method in the CALYPSO packages.^{4,5} The flowchart of the SPAI method in CALYPSO is presented in Fig. 3. First, the initial structures are randomly generated with physical constraints that include symmetry and minimal interatomic distances. Fingerprint function^{4,32} is adopted to quantify similarities of the new structure with all the previous ones. If the structure is similar to any one of the previous structures, it will be discarded and replaced by a newly generated one. After all the structures are generated, variable-cell geometry relaxations are performed to drive the structure energy to the local minimum. Then, all the structures of this generation will be ranked by fitness (e.g., total energy). In the next generation, the SPAI method will be adopted to generate the new structures. These steps are iterated until a termination criterion (such as a prescribed threshold or a fixed number of iterations) is attained.

III. RESULTS AND DISCUSSION

Our method has been benchmarked by the prediction of three known structures of $MgAl_2O_4$, $SrTiO_3$, and $Mg_3Al_2Si_3O_{12}$ having 28, 50, and 160 atoms in the lattice cells, respectively. The results are listed in Table I and compared with the results derived from the simulation runs using the previously developed local particle swarm optimization (LPSO) method.⁴ Both schemes precisely reproduced the experimental structures of $MgAl_2O_4$ and $SrTiO_3$ with a success rate of 100%; however, the SPAI method is more efficient than the LPSO method⁴ as the average number of structures required to identify the true structure is much reduced.

The efficiency of the current SPAI is comparable to other popular algorithms. For example, 332 structure samplings are required to find the ground state structure of $SrTiO_3$ using the SPAI method, which is less than that required by other methods.^{25,33} Furthermore, it is evident that SPAI has excellent performance for the complex structure of $Mg_3Al_2Si_3O_{12}$, where the earlier approach fails without a biased input of experimental cell parameters in the simulation.²⁵ The current method has a high success rate of 100% in stark contrast to the low success rate of 20% without any constraint of cell parameters for LPSO. It is also noteworthy that the average number of structures required to achieve the experimental structure

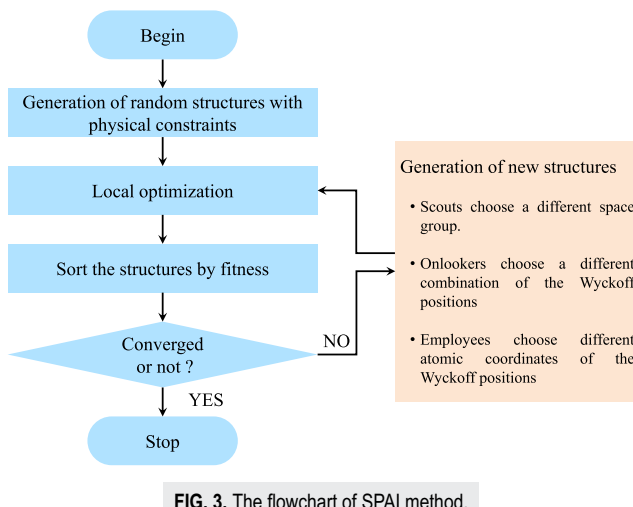


FIG. 3. The flowchart of SPAI method.

TABLE I. Simulation results for $MgAl_2O_4$, $SrTiO_3$, and $Mg_3Al_2Si_3O_{12}$ derived from SPAI and LPSO algorithms without any constraint of cell parameters. 50 different structure prediction runs are performed for each system where the population per generation contains 50 structures and the maximum number of generations is set to be 100. N denotes the average number of structures required to identify the experimental structures of $MgAl_2O_4$, $SrTiO_3$, and $Mg_3Al_2Si_3O_{12}$ for 50 different runs. The number of atoms in the unit cell is given in the parentheses below each system.

Systems (No. of atoms)	Methods	N	Success rate (%)
$MgAl_2O_4$ (28)	LPSO	652	100
	SPAI	358	100
$SrTiO_3$ (50)	LPSO	809	100
	SPAI	332	100
$Mg_3Al_2Si_3O_{12}$ (160)	LPSO	1693	20
	SPAI	393	100

TABLE II. The energies of BLJM-60, BLJM-80, and BLJM-256 structures predicted by SPAI, MH, and BH. ϵ_{AA} is the potential well depth of the type A atom.

BLJM	SPAI	MH ¹⁴	BH ³⁶
60	-7.50	-7.49	-7.08
80	-7.52	-7.50	-7.33
256	-7.47	-7.43	-7.20

for the current method is amazingly small at 393 for such a complex system.

To demonstrate the capability of our method for applications of complex systems, we applied it to predict the plausible crystalline structures of $\text{Ba}_{1.6}\text{Ca}_{2.3}\text{Y}_{1.1}\text{Fe}_5\text{O}_{13}$,³⁴ which have been synthesized by experiments.³⁵ Our approach successfully reproduced the plausible ordered structure of $\text{Ba}_2\text{Ca}_2\text{Y}\text{Fe}_5\text{O}_{13}$ containing 92 atoms in simulated cells proposed by experiments³⁵ without the requirements of prior experimental knowledge, validating the effectiveness of our approach for applications to compositionally complex materials.

Due to highly frustrated PES, identifications of the ground state crystalline structures of binary Lennard-Jones mixtures (BLJMs) pose a great challenge.^{14,36} Our approach is performed to determine the global minima for BLJMs containing 60, 80, and 256 atoms. The predicted structures are energetically more favorable than those found by minima hopping (MH)¹⁴ and basin-hopping (BH),³⁶ as illustrated in Table II. These structures share similar layered structural features (Fig. S3), which consist of simple close-packed layers formed purely of A atoms and unexpectedly complex polyhedral layers formed by mixtures of A and B. It is notable that the unit cell dimension of the predicted structure of BLJM-256 is amazingly large over 97 Å. These results demonstrate that our approach holds

a promise for applications to the complex structures of large systems containing more than 100 atoms.

It is expected that the crystalline structure of ice displays enormous complexity with a large unit cell because of the existence of the complex behavior of hydrogen order/disorder. Two structure predictions of ice with simulation cells containing 48 and 144 atoms per unit cell were performed at 10 GPa using the new method and LPSO method as implemented in the CALYPSO code.⁴ The developed method successfully reproduces the experimentally observed $I4_1amd$ structure and has higher efficiency as evidenced by the fact that 208 optimized structures are required to identify the experimental structure of ice,³⁷ which is less than that of LPSO (>750 structures). Furthermore, the developed method offers a new structure of $Fddd$ with the distinctive orientations of H_2O molecules compared with the known $I4_1amd$ structure [Fig. 4(a)]. The new structure contains 144 atoms per unit cell. The static energy of $Fddd$, calculated using density functional theory within the Perdew–Burke–Ernzerhof functional at 0 K, is higher than that of the $I4_1amd$ by only 2.0 meV/atom. The Gibbs free energies of the $Fddd$ and $I4_1amd$ are calculated within a quasi-harmonic approximation with respect to the temperature up to 1000 K. It clearly shows that the stabilization of the $Fddd$ structure is energetically more favorable than $I4_1amd$ at a temperature of 600 K [Fig. 4(b)].

Although this work is focused on the development of structure prediction on three-dimensional (3D) crystals, the proposed STG is also expected to be equally efficient for the prediction of other structures (e.g., zero-, one-, and two-dimensional structures). Since there are only 17 planar or 80 layer groups and 75 rod groups for 2D and 1D structures, respectively, structure searching simulation might be much easier. For a 0D isolated structure, point groups are used for the symmetry description, but have an infinite number. Here, the use of certain point groups, C_2 , C_s , and C_{2v} , is expected to be useful.

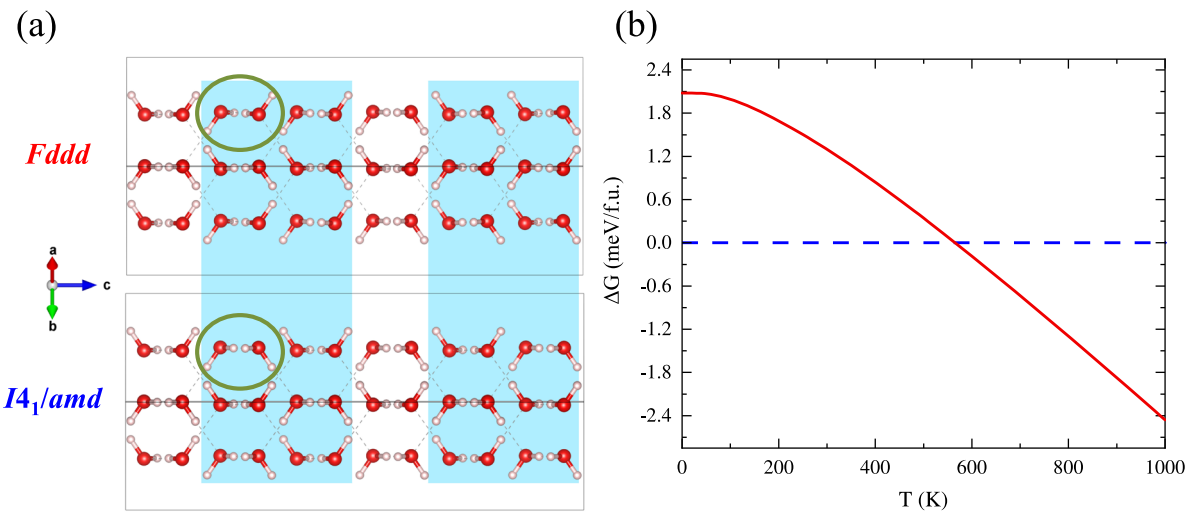


FIG. 4. (a) The new predicted structure with a space group of $Fddd$ containing 144 atoms in comparison with the stable $I4_1amd$ structure with a $\sqrt{2} \times \sqrt{2} \times 3$ supercell. (b) The calculated difference of Gibbs free energies of $Fddd$ with respect to $I4_1amd$ at a harmonic approximation level as function of temperature up to 1000 K.

IV. CONCLUSION

In summary, we have developed a CSP method by the introduction of the hierarchical symmetry tree graph combined with a biased symmetry-adapted artificial intelligence algorithm. The approach drives the structure search toward the global minimum by fast identification of the most promising subsets and further in-depth exploitation. The performance of the proposed method has been demonstrated by applications to the structural complex systems of BLJMs and ice, which contain hundreds of atoms per simulated cell. As available computational resources are increased in the future, it would be expected that our method can be widely applied in the theoretical treatment of compositionally and structurally complex structures with large unit sizes containing thousands of atoms.

SUPPLEMENTARY MATERIAL

See the [supplementary material](#) for the details of the method and calculations and information of predicted structures.

ACKNOWLEDGMENTS

This research was supported by the National Key Research and Development Program of China under Grant No. 2016YFB0201201; the National Natural Science Foundation of China under Grant Nos. 12034009, 91961204, 11774127, 12174142, 11404128, 11822404, 11534003, and 11974134; the Program for JLU Science and Technology Innovative Research Team. Part of the calculation was performed in the high-performance computing center of Jilin University.

AUTHOR DECLARATIONS

Conflict of Interest

The authors have no conflicts to disclose.

Author Contributions

X.S. and J.L. contributed equally to this work.

DATA AVAILABILITY

The data that support the findings of this study are available within the article and its [supplementary material](#).

REFERENCES

- ¹J. Nocedal and S. Wright, *Numerical Optimization* (Springer Science & Business Media, 2006).
- ²S. T. Call, D. Y. Zubarev, and A. I. Boldyrev, “Global minimum structure searches via particle swarm optimization,” *J. Comput. Chem.* **28**, 1177–1186 (2007).
- ³C. J. Pickard and R. J. Needs, “Ab initio random structure searching,” *J. Phys.: Condens. Matter* **23**, 053201 (2011).
- ⁴Y. Wang, J. Lv, L. Zhu, and Y. Ma, “CALYPSO: A method for crystal structure prediction,” *Comput. Phys. Commun.* **183**, 2063–2070 (2012).
- ⁵Y. Wang, J. Lv, L. Zhu, and Y. Ma, “Crystal structure prediction via particle-swarm optimization,” *Phys. Rev. B* **82**, 094116 (2010).
- ⁶B. Gao, P. Gao, S. Lu, J. Lv, Y. Wang, and Y. Ma, “Interface structure prediction via CALYPSO method,” *Sci. Bull.* **64**, 301–309 (2019).
- ⁷Y. Forman and M. Cameron, “Modeling aggregation processes of Lennard-Jones particles via stochastic networks,” *J. Stat. Phys.* **168**, 408–433 (2017).
- ⁸A. R. Oganov, “Crystal structure prediction: Reflections on present status and challenges,” *Faraday Discuss.* **211**, 643–660 (2018).
- ⁹Y. Wang and Y. Ma, “Perspective: Crystal structure prediction at high pressures,” *J. Chem. Phys.* **140**, 040901 (2014).
- ¹⁰F. Peng, Y. Sun, C. J. Pickard, R. J. Needs, Q. Wu, and Y. Ma, “Hydrogen clathrate structures in rare earth hydrides at high pressures: Possible route to room-temperature superconductivity,” *Phys. Rev. Lett.* **119**, 107001 (2017).
- ¹¹H. Liu, I. I. Naumov, R. Hoffmann, N. W. Ashcroft, and R. J. Hemley, “Potential high- T_c superconducting lanthanum and yttrium hydrides at high pressure,” *Proc. Natl. Acad. Sci. U. S. A.* **114**, 6990–6995 (2017).
- ¹²S. P. Brooks and B. J. T. Morgan, “Optimization using simulated annealing,” *Statistician* **44**, 241 (1995).
- ¹³D. J. Wales and J. P. K. Doye, “Global optimization by basin-hopping and the lowest energy structures of Lennard-Jones clusters containing up to 110 atoms,” *J. Phys. Chem. A* **101**, 5111–5116 (1997).
- ¹⁴M. Amsler and S. Goedecker, “Crystal structure prediction using the minima hopping method,” *J. Chem. Phys.* **133**, 224104 (2010).
- ¹⁵R. Martoňák, A. Laio, and M. Parrinello, “Predicting crystal structures: The Parrinello-Rahman method revisited,” *Phys. Rev. Lett.* **90**, 075503 (2003).
- ¹⁶S. M. Woodley, P. D. Battle, J. D. Gale, and C. A. Catlow, “The prediction of inorganic crystal structures using a genetic algorithm and energy minimisation,” *Phys. Chem. Chem. Phys.* **1**, 2535–2542 (1999).
- ¹⁷A. R. Oganov and C. W. Glass, “Crystal structure prediction using *ab initio* evolutionary techniques: Principles and applications,” *J. Chem. Phys.* **124**, 244704 (2006).
- ¹⁸N. L. Abraham and M. I. J. Probert, “A periodic genetic algorithm with real-space representation for crystal structure and polymorph prediction,” *Phys. Rev. B* **73**, 224104 (2006).
- ¹⁹G. Trimarchi and A. Zunger, “Global space-group optimization problem: Finding the stablest crystal structure without constraints,” *Phys. Rev. B* **75**, 104113 (2007).
- ²⁰D. C. Lonie and E. Zurek, “XTALOPT version r7: An open-source evolutionary algorithm for crystal structure prediction,” *Comput. Phys. Commun.* **182**, 2305–2306 (2011).
- ²¹A. R. Oganov, C. J. Pickard, Q. Zhu, and R. J. Needs, “Structure prediction drives materials discovery,” *Nat. Rev. Mater.* **4**, 331–348 (2019).
- ²²T. H. Cormen, C. E. Leiserson, R. L. Rivest, and C. Stein, *Introduction to Algorithms* (MIT Press, 2009).
- ²³C. P. Massen and J. P. Doye, “Power-law distributions for the areas of the basins of attraction on a potential energy landscape,” *Phys. Rev. E* **75**, 037101 (2007).
- ²⁴D. J. Wales, “Symmetry, near-symmetry and energetics,” *Chem. Phys. Lett.* **285**, 330–336 (1998).
- ²⁵A. O. Lyakhov, A. R. Oganov, H. T. Stokes, and Q. Zhu, “New developments in evolutionary structure prediction algorithm USPEX,” *Comput. Phys. Commun.* **184**, 1172–1182 (2013).
- ²⁶C. E. Mohn, S. Stolen, and W. Kob, “Predicting the structure of alloys using genetic algorithms,” *Mater. Manuf. Processes* **26**, 348–353 (2011).
- ²⁷J. Zhang and M. Dolg, “ABCcluster: The artificial bee colony algorithm for cluster global optimization,” *Phys. Chem. Chem. Phys.* **17**, 24173–24181 (2015).
- ²⁸J. Zhang and M. Dolg, “Global optimization of clusters of rigid molecules using the artificial bee colony algorithm,” *Phys. Chem. Chem. Phys.* **18**, 3003–3010 (2016).
- ²⁹O. Yañez, R. Báez-Grez, D. Inostroza, W. A. Rabanal-León, R. Pino-Ríos, J. Garza, and W. Tiznado, “AUTOMATON: A program that combines a probabilistic cellular automata and a genetic algorithm for global minimum search of clusters and molecules,” *J. Chem. Theory Comput.* **15**, 1463–1475 (2018).
- ³⁰P. Avery and E. Zurek, “RandSpg: An open-source program for generating atomistic crystal structures with specific spacegroups,” *Comput. Phys. Commun.* **213**, 208–216 (2017).

- ³¹S. Fredericks, K. Parrish, D. Sayre, and Q. Zhu, "PyXtal: A python library for crystal structure generation and symmetry analysis," *Comput. Phys. Commun.* **261**, 107810 (2021).
- ³²L. Zhu, M. Amsler, T. Fuhrer, B. Schaefer, S. Faraji, S. Rostami, S. A. Ghasemi, A. Sadeghi, M. Grauzintyte, C. Wolverton *et al.*, "A fingerprint based metric for measuring similarities of crystalline structures," *J. Chem. Phys.* **144**, 034203 (2016).
- ³³Z. Falls, P. Avery, X. Wang, K. P. Hilleke, and E. Zurek, "The XtalOpt evolutionary algorithm for crystal structure prediction," *J. Phys. Chem. C* **125**, 1601–1620 (2020).
- ³⁴A. Demont, M. S. Dyer, R. Sayers, M. F. Thomas, M. Tsiamtsouri, H. N. Niu, G. R. Darling, A. Daoud-Aladine, J. B. Claridge, and M. J. Rosseinsky, "Stabilization of a complex perovskite superstructure under ambient conditions: Influence of cation composition and ordering, and evaluation as an SOFC cathode," *Chem. Mater.* **22**, 6598–6615 (2010).
- ³⁵M. S. Dyer, C. Collins, D. Hodgeman, P. A. Chater, A. Demont, S. Romani, R. Sayers, M. F. Thomas, J. B. Claridge, G. R. Darling, and M. J. Rosseinsky, "Computationally assisted identification of functional inorganic materials," *Science* **340**, 847–852 (2013).
- ³⁶T. F. Middleton, J. Hernández-Rojas, P. N. Mortenson, and D. J. Wales, "Crystals of binary Lennard-Jones solids," *Phys. Rev. B* **64**, 184201 (2001).
- ³⁷K. Umemoto and R. M. Wentzcovitch, "Theoretical study of the isostructural transformation in ice VIII," *Phys. Rev. B* **71**, 012102 (2005).